A comparative evaluation of equivalent circuit and finite element electrical skin modelling techniques

T Greig[1], K Yang[2] and R Torah[1]

[1] School of Electronics and Computer Science, University of Southampton, UK, SO17 1BJ

[2] Winchester School of Art, University of Southampton, UK, SO23 8DL

E-mail: tg8g16@soton.ac.uk

Abstract. Mathematical models are essential to our understanding of the electrical properties of the skin. In this paper, two types of simulation model, an equivalent circuit and a finite element simulation were investigated and compared to evaluate their accuracy. Impedance spectra were measured, between 100 Hz and 50 MHz, (the limits of the available spectrum analyser) of a pair of electrodes placed on skin and these spectra used to find the parameters of a standard equivalent circuit model. The resulting indicated that the components of the equivalent circuit may represent different parts of the skin physiology that indicated by the literature.

A simulation model was constructed in COMSOL, with the dimensions, permittivity and conductivity of each skin layer taken from across the published literature. This model was tested for sensitivity to the thicknesses of tissue layers as well as the shape of the boundary between layers. It was found that changing the layer thicknesses only had a significant effect for the *stratum corneum* and dermis, and that changing the shape of the boundary between layers created an impedance change of up to two times at certain higher frequencies (> 1 kHz).

While the impedance curves generated by the two models had the same overall profile, there was a difference of up to 100 times in their DC impedance values. This indicated that the broad understanding of how electrical signals of different frequencies pass through the skin is correct, but that significant insufficiencies exist in the published properties of the skin layers, particularly the *stratum corneum* and that finding more accurate values for these properties is necessary for the development of better models.

Finite Element Modelling, Equivalent Circuit Modelling, Skin

Submitted to: *Biomed. Phys. Eng. Express*

1. Introduction

Knowledge of the electrical properties of the skin is crucial to the effectiveness of several medical treatments. Stimulation treatments such as functional electrical stimulation (FES) and transcutaneous electrical nerve stimulation (TENS) are widely used in stroke rehabilitation and pain relief respectively. Electrocardiograms (ECGs), electroencephalograms (EEGs) and other biopotential monitoring systems are used in the diagnosis and monitoring of numerous conditions. These treatments all require an understanding of the electrical behaviour of the skin to be effective (Neuman 2010).

In the context of ECG monitoring, for example, Taji, Shirmohammadi, Groza & Batkin (2014) show the input error to an ECG amplifier is proportional to the impedance of the source and thus, when compensating for this, errors in the estimation of this impedance will produce a corresponding error in the result. Most biopotential measurement systems also use differential measurements between two or more electrodes (Spinelli et al. 2003, Tankisi et al. 2020). To ensure such measurements are accurate, the input impedance at each electrode must be the same so the factors that influence this impedance must be understood so that they can be controlled.

Relying on physical measurements alone, it is difficult to gain an understanding of how electric current passes through the skin: it requires the insertion of needle electrodes into a test subject which can be painful and only gives data at a few specific points. For systems such as skin, which are hard to observe, mathematical models and simulations are a crucial way of developing a more complete understanding. Unlike physical measurements, they can provide detailed information about any point within their scope and can be used to rapidly evaluate stimulation or measurement systems without the need for physical fabrication or testing.

The weakness of modelling is that the results can be less accurate than those from a physical experiment. A model will never perfectly match the real equivalent, particularly with a system as complex as biological tissue.

There are two main approaches available for modelling the electrical behaviour of the skin: the first is to use an equivalent circuit model, wherein the different layers of tissue are represented by combinations resistors, capacitors and inductors, which present an equivalent impedance (Assambo et al. 2007). The second is to use a tool such as finite element analysis to simulate a full, three dimensional model of the tissue layers, using their dimensions and the electrical properties of their materials (Hartinger et al. 2010).

Equivalent circuit models have the advantage of greater simplicity; having fewer parameters means that their values can be derived from simple physical measurements. However, equivalent circuits are less detailed; they provide no information about the flow of current within a tissue layer, only what the electrical potential is on either side. They are also harder to generalise; the equivalent circuit model for two electrodes 5 cm apart cannot be easily converted into one for electrodes 10 cm apart, for example.

A 3D simulation model solves these problems by including the geometry of the

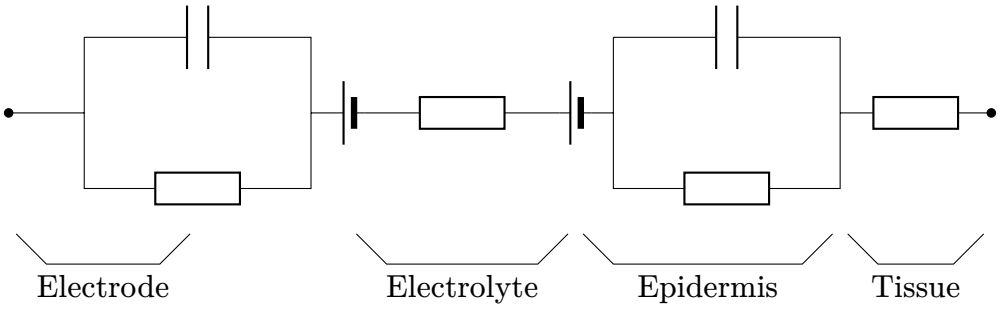

Figure 1. Neuman's equivalent circuit model of a skin – electrode system including the external electrode, electrolyte, epidermis and underlying tissue (Neuman 2010).

tissue layers in its simulation and by having that geometry specified separately from the material properties. These added degrees of freedom come with the drawback of making the model more challenging to derive.

An equivalent circuit model that has been widely used in the field of biopotential monitoring (Assambo et al. 2007, Taji, Shirmohammadi & Groza 2014, Xiong et al. 2019) was derived in 1989 by Kaczmarek and Webster (Kaczmarek & Webster 1989) before being further developed and matched to the physiology of the skin by Neuman (Neuman 2010). This model is shown in figure 1. Kaczmarek and Webster's equivalent circuit consisted of a second order filter of two, parallel resistor – capacitor networks plus an additional series resistance. The first of these RC pairs was attributed by Neuman to the double layer impedance at the interface between the electrode and the electrolyte (either sweat or an applied gel interface), the capacitance being generated by the accumulation of charge between the ionically conducting electrolyte and the electrically conducting electrode, and the resistor representing the leakage resistance across that boundary. The second RC pair is attributed to the epidermis, the upper layers of the skin. The electrolyte itself and the tissue layers below the epidermis are considered to be purely resistive.

Neuman also adds two potentials, represented as cells in figure 1, one caused by the half-cell between the electrode and the electrolyte, and one caused by the *stratum corneum* (the top part of the epidermis, consisting of devitalised cells), which acts as a semi-permeable membrane, creating a difference in ion concentration.

The most significant inaccuracy remaining in this model is the presumption that the interfaces and tissues present ideal capacitances. Factors including the inhomogeneity of the tissues (Hartinger et al. 2010, Huclova et al. 2010) and the polar nature of water molecules (Schwan 1957) cause the effective capacitance to change at different frequencies. These are referred to as dispersion effects. There are three main dispersion effects, labelled α, β and γ, which occur at around 10^2, 10^6 and 10^{11} Hz respectively (Schwan 1957).

A number of different ways of mathematically representing these effects have been proposed. One of the simplest is the impedance based version (Brown et al. 1999) of the Cole-Cole equation (Cole & Cole 1942). In this method, the impedance of a

capacitor is changed from $(j\omega C)^{-1}$ to $(j\omega C)^{\alpha-1}$ where α is a parameter between 0 and 1 (of no particular relation to the α dispersion effect). With this modification, the circuit in figure 1 becomes a sufficiently accurate model to be fit to recorded impedance data.

In order to create a 3D simulation of the skin, it is necessary to find the thicknesses of each layer as well as their electrical properties: their conductivity and permittivity. The thickness of each skin layer is well established, being measurable with relative ease using microscopy techniques (Lee & Hwang 2002, Holbrook & Odland 1974). Identifying the permittivity and conductivity is much more difficult.

Most of the published data on tissues' electrical properties is the result of measurements using open ended, coaxial probes (Gabriel, Gabriel & Corthout 1996, Birgersson et al. 2013). The coaxial line is butted against the sample and the S_{11} reflection coefficient is measured using a network analyser (Stuchly & Stuchly 1980). From this, the complex permittivity, a value that represents both permittivity and conductivity, can be derived (Schwan 1957). The depth into the sample that the electric field penetrates can be controlled by varying the inner and outer diameters of the coaxial probe (Lahtinen et al. 1997).

To get an accurate measurement of an individual skin layer, it is necessary to have the electric field pass through just that layer. For the layers at the top of the skin, this can be challenging as their shallow depth makes them difficult to isolate (Martinsen et al. 1997).

This work consists of the creation of two models of the skin: one based around an equivalent circuit, with parameters derived from physical measurements; the other using finite element analysis software with parameters reported in the literature. The simulations from these two models are then compared to identify potential inaccuracies.

2. The Equivalent Circuit Model

2.1. Equivalent Circuit Model Derivation Method

The equivalent circuit model of the skin was created by fitting the circuit model described above to measured impedance spectra.

Bespoke carbon rubber electrodes, made from Fabinks E-0003 carbon paste, were used to collect these measurements. Silver connections (Fabinks TC-C4007) and a polyurethane interface (Fabinks UV-IF-1004) were dispenser printed onto a polyester–cotton backing using the dispenser printing method described in (Liu et al. 2022). A 28×28 mm, carbon rubber pad was then stencil printed on top (Liu et al. 2019), giving it a thickness of 2 mm.

Impedance measurements were taken using a Wayne Kerr 6550B impedance analyser. This was capable of recording both the magnitude and phase of the impedance connected to it within a range of 100 Hz to 50 MHz. When making

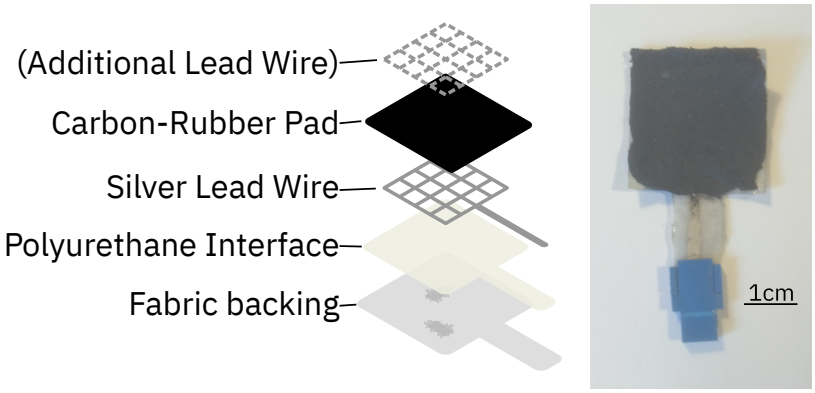

Figure 2. Electrodes used for physical measurements in this paper. The printed electrodes consisted of a polyester–cotton base, a layer of polyurethane interface, a silver printed lead wire and a carbon rubber pad. A second set of electrodes were printed with an extra silver grid on top, to measure the impedance of the electrode pad alone.

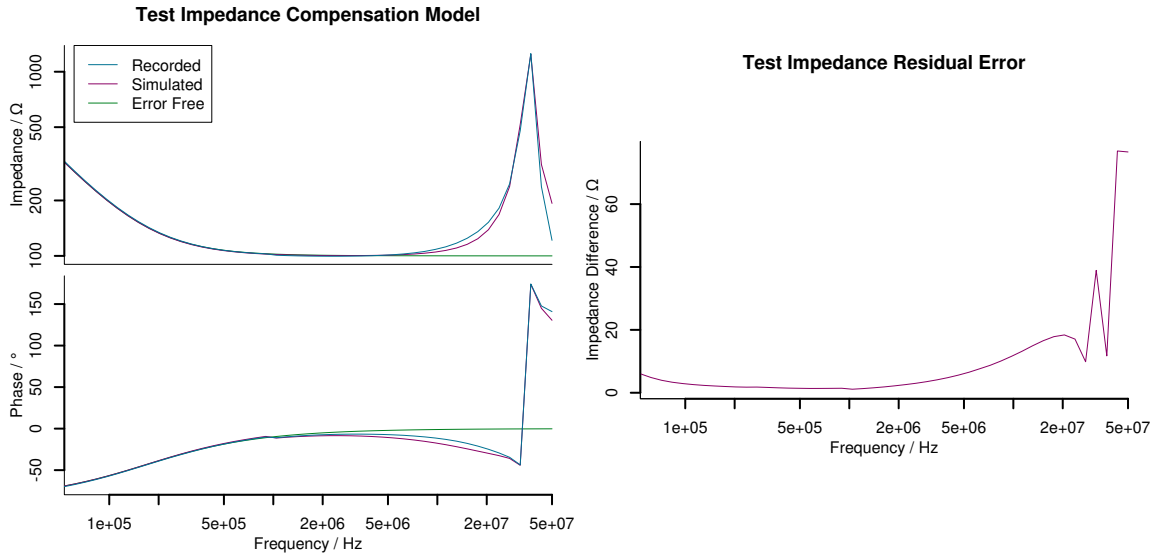

Figure 3. Left: Recorded impedance (blue) and true impedance with the expected error included (purple) when measuring a circuit consisting of a 100 Ω resistance in series with a parallel 100 kΩ resistance and a 10 nF capacitance. The theoretical impedance of these components, were there no error, is shown in green. Right: The residual error after compensation, equivalent to the difference between the blue and purple lines on the left hand graph.

measurements above 1 MHz, the analyser's output included an additional equipment error, equivalent to a parallel resistor, inductor and capacitor as well as a fixed time delay added to the phase, see figure 3. This persisted after running the manufacturer recommended calibration procedure but was consistent enough that it could be reliably removed from the data after exporting using equation 1.

$$Z_{true} = \left(Z_{measured} - \left(R^{-1} + \left(\frac{1}{\mathrm{j}\omega C} \right)^{-1} + (\mathrm{j}\omega L)^{-1} \right)^{-1} \right) \times \mathrm{e}^{-\mathrm{j}\omega t \times (f > 1\mathrm{MHz})}, \\ t = 4.61\mathrm{ns}\ (\sigma = 0.2\mathrm{ns}),\ R = 35\mathrm{k}\Omega\ (\sigma = 2\mathrm{k}\Omega), \\ C = 25.4\mathrm{pF}\ (\sigma = 1.0\mathrm{pF}),\ L = 603\mathrm{nH}\ (\sigma = 49.1\mathrm{nH}) \tag{1}$$

Before attempting to measure the properties of the skin, a series of tests were conducted, identifying the properties of the electrodes themselves. The first of these, designed to measure the impedance of just the electrode's carbon pad, used a duplicate electrode, fabricated as described above, but with an additional lead wire printed on top of the pad as well as behind it. This allowed the impedance of just the carbon rubber to be measured, with minimal effects from connection interfaces. Such measurements were taken with 0, 50, 100 and 150 g masses compressing the electrode.

Following this, the impedance between a normal, single lead wire electrode and a copper sheet was measured. This gave an insight into the interface impedance between the electrode and the surface it is contacting. The impedance between the electrode and the copper was tested with 3 different masses applied: 50, 100 and 150 g, and with the interface both wet and dry. During wet tests, 0.05 ml of tap water was applied to the electrode surface using a syringe. This was enough that, under a 150 g mass, small amounts of water could be seen seeping out from the sides. This test was performed independently with two different electrodes: A and B, that would later be used together for measuring the tissue. These two electrodes were produced using the same method but due to variations in the materials and the texture of the electrode surface, could have had slightly different properties and so were tested separately.

These measurements were fit to the electrode and electrolyte sections of the equivalent circuit shown in figure 1. Because only the impedance was being considered, the electrode – electrolyte half-cell potential was ignored. The R language's non-linear least squares routine (R Core Team 2022) was used to find the parameters to equation 2 which best matched the recorded impedance curves, where R_S is the series resistance, R_P the parallel resistance, and C_P and α the properties of the capacitor.

$$Z = R_S + \frac{1}{\frac{1}{R_P} + (\mathrm{j}\omega C_P)^{1-a}} \tag{2}$$

The tests on skin were performed similarly, with 50, 100 or 150 g of mass and dry or with 0.05 ml of water, on each electrode. When testing on skin, it was ensured that tests under dry conditions were performed first so that any moisture added during the wet tests wouldn't soak into the skin and affect them. When conducting wet tests, water was applied to the subject's skin using a syringe. The electrodes were then placed on top and held in place using first the 50 g mass, then the 100 and 150 g. Each time the electrodes were repositioned, both the electrode surface and the subject's skin were dried with a paper towel and water was reapplied. The electrodes were placed 30, 50, 70 and 90 mm apart, centre to centre, in turn, on the ventral forearm. The bias applied by the impedance meter while measuring was 1 V so was not perceptible to

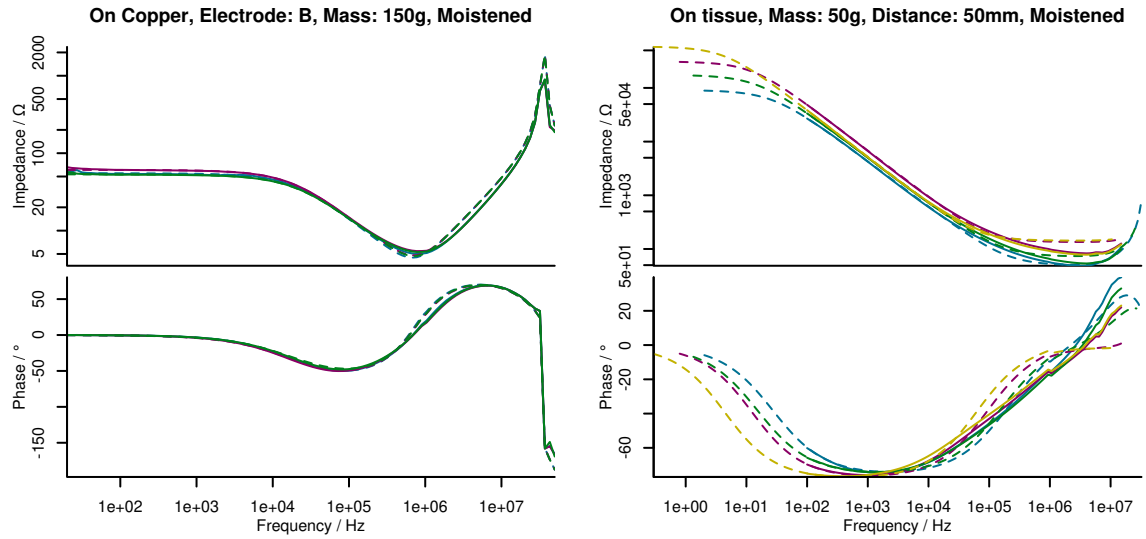

Figure 4. Recorded (solid) and fitted (dashed) impedance curves. The different colours are multiple repeats of the same measurement. The graph on the left is from measuring the impedance between a single electrode and copper sheet. The graph on the right is the impedance between two electrodes placed 50 mm apart on the ventral forearm.

the subject, and wouldn't affect the electrical properties of the skin by its application (Pliquett et al. 1995).

Because the recorded impedance was approximately three orders of magnitude higher in these measurements than in the ones conducted on copper, and because there was no sign on the impedance curve of a second break frequency, the impedance recorded on skin was fitted against just the epidermis and tissue sections of figure 1. Again, the half-cell potential was ignored.

2.2. Equivalent Circuit Model Results

Measurements of the properties of the two–lead–wire electrodes revealed that the bulk of the electrodes' pads presented a purely resistive impedance of no more than 5 Ω. This was consistent across the entire frequency range and did not change with the amount of mass applied.

The fitted model parameters derived from electrodes on copper are shown in figure 5. Contrary to the predictions of the model in figure 1 the parallel resistance and capacitance behave as if they were not entirely being produced by the electrode–electrolyte boundary, but at least in part by the electrolyte beneath them. The appearance of a capacitance in the dry tests, when no double–layer producing electrolyte is present, shows that a capacitance can arise directly between the electrode and the skin. The positive correlation with mass corroborates this; as more mass is applied, the electrode and skin will move closer together, decreasing the dielectric width and increasing capacitance. These results show that moistening the electrodes

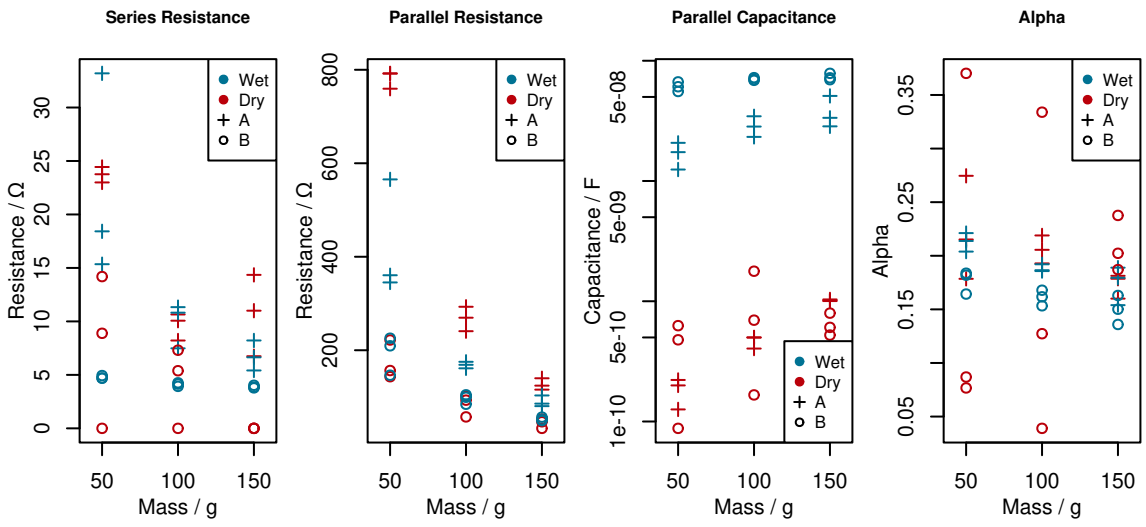

Figure 5. Fitted model parameters for electrodes placed on a copper sheet. The data points come from independently fitting to three repeats of each measurement. Note that the capacitance is given on a logarithmic scale as the result for that parameter occupies such a large range.

increases the capacitance by approximately two orders of magnitude. This is close to the difference between the relative permittivities of water and air (a factor of 80 at room temperature (Archer & Wang 1990)), implying that a significant portion of the capacitance recorded in the moistened cases is across the whole electrolyte as well.

The parallel resistance shows a pronounced negative correlation with the applied mass. This was not observed in the electrode pads themselves when measured alone, but could be expected from an electrolyte space decreasing in thickness as more pressure is applied. Likewise, the capacitance shows a slight increase with increasing pressure, as the distance between the conductive regions of carbon rubber and copper is decreased.

The derived series resistance values show a wide variation in a way that does not correlate well with either dampness or applied mass. The reason for these variable results has to do with how series resistance is extracted from an impedance curve. The series resistance is found by looking at the value at which the impedance becomes constant at high frequencies. In this case though, because of the meter's built in error, the impedance magnitude starts increasing again before this can happen. The result of this is that the series resistance never becomes the dominant impedance in the circuit and so it cannot be measured accurately.

The one configuration that produced a consistent result for series impedance was the measurement of electrode B with a wet interface (the blue circles in figure 5). The constant resistance of just under 5 Ω for all applied masses matches the measurements of the electrode pad alone, implying that the series resistance originates mostly from within the electrode. However, the variability of the results from other configurations

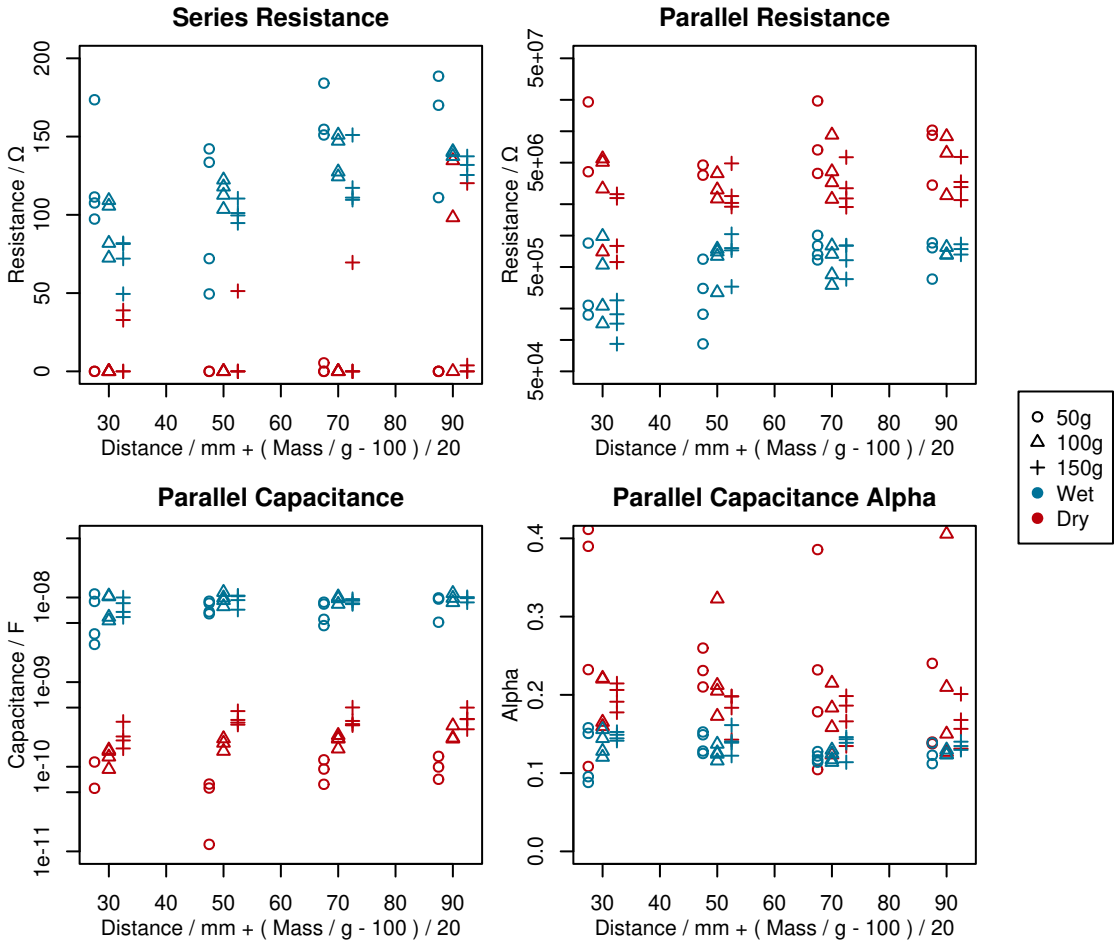

Figure 6. Fitted model parameters for a pair of electrodes on tissue. The x axes primarily plot the distance between the electrodes, however, to also show the effect of changing mass, measurements taken under 50 g are shown the equivalent of 2.5 mm left of their true position, and those with 150 g, 2.5 mm to the right, despite all having been measured at the same set of distances.

means that this cannot be stated with confidence.

The fitted model parameters for the tissue are shown in figure 6. For the same reason as previously, series resistance values, particularly for dry configurations, show a wide variation, even within repeats of the same measurement. The wet measurements, by virtue of their higher capacitance and lower parallel resistance, did exhibit a frequency range at which the series resistance was the dominant contribution to the overall impedance, allowing it to be measured more reliably in these cases. The model in figure 1 ascribes the series resistance to the deeper tissues below the skin. Were this the case, the measured series resistance values would be expected to have a direct, linear correlation with distance. While the resistance value does increase in an approximately linear fashion, the constant offset along with the decrease induced by higher masses, implies there is a significant contribution from the upper layers of the skin and the interface from the electrodes as well.

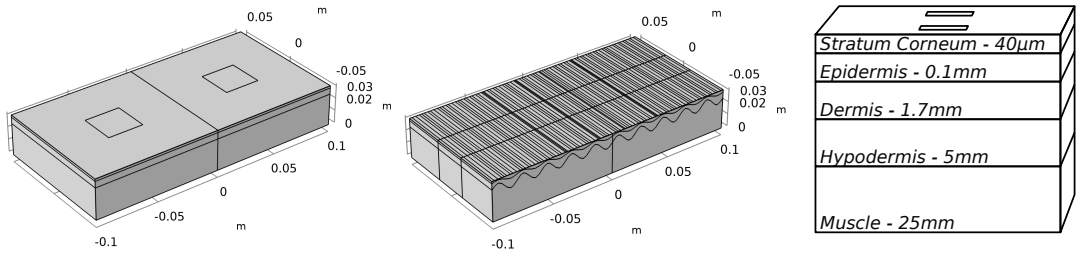

Figure 7. Basic version of the COMSOL simulation model (left) and version with uneven layer boundaries (centre). The image on the right shows how each layer of the skin was represented by a layer in the model.

The parallel resistance and capacitance values behave as the model predicts. Showing no correlation with distance is consistent with their being sourced from the upper layers of the skin. The increase in capacitance and decrease in resistance when the electrodes are wet is to be expected as well: the majority of the epidermis' impedance comes from the *stratum corneum*, the layer of dry, dead cells that make up the outer most layer of the skin. Applied water will get absorbed by this layer, increasing both its conductivity and permittivity.

Taken together, these results imply that the impedance of the skin – electrode system is equivalent to that presented in figure 1. However the physical source of each component of that impedance appears to differ from those given in the literature.

3. The Finite Element Skin Model

3.1. Finite Element Model Construction

Finite element analysis is a simulation methodology that works by breaking a system down into small sections, then solving a set of equations for each section using numerical methods. To verify the accuracy of the equivalent circuit model described above, a finite element simulation model was created using the modelling software COMSOL (COMSOL Inc. Stockholm, Sweden).

This model, shown in figure 7 (left), consisted of five layers, representing the *stratum corneum*, the epidermis, the dermis, the hypodermis and the muscle. The electrical properties of each layer were taken from values published in the literature and are shown in table 1. The data for the *stratum corneum* is specific to the ventral forearm (Yamamoto & Yamamoto 1976), the other layers' data is for generic skin.

Where available, the properties of the Cole–Cole dispersion equation are used. As opposed to the impedance version used in the physical modelling above, this version of the equation, (3), calculates the complex permittivity of a material as a function of frequency. This value can then be split into permittivity and conductivity according to equation 4 (Gabriel, Lau & Gabriel 1996).

$$\epsilon^*(\omega) = \epsilon_\infty + \sum_n \frac{\Delta\epsilon_n}{1 + (\mathrm{j}\omega\tau_n)^{(1-\alpha_n)}} + \frac{\sigma_i}{\mathrm{j}\omega\epsilon_0} \tag{3}$$

Tissue	ε_∞	$\Delta\varepsilon_n$	τ_n / s	α_n	σ_i / S/m	Depth / mm
Stratum Corneum	100	1400 1×10^4	5.3×10^{-7} 1.59×10^{-2}	0.05 0.4	1.3×10^{-5}	0.04
Epidermis	$\epsilon_r = 1.14 \times 10^3$, $\sigma = 0.55\,S/m$					0.1
Dermis	$\epsilon_r = 1.14 \times 10^3$, $\sigma = 2.9\,S/m$					1.7
Hypodermis	5.5	15 2×10^5 1×10^7	15.92×10^{-9} 159.15×10^{-6} 7.95×10^{-3}	0.2 0.05 0.01	0.01	5
Muscle	54	7000 1.2×10^6 2.5×10^7	353.86×10^{-9} 318.83×10^{-6} 2.274×10^{-3}	0.1 0.1 0	0.2	25

Table 1. Electrical parameters and depths of the stratum corneum (Yamamoto & Yamamoto 1976), epidermis and dermis (Li 2018), hypodermis and muscle (Gabriel, Lau & Gabriel 1996).

$$\epsilon^*(\omega) = \epsilon_r - \frac{\mathrm{j}\sigma}{\omega\epsilon_0} \tag{4}$$

The data for the stratum corneum was collected using electrodes with a gel interface (Yamamoto & Yamamoto 1976), meaning this model corresponds best to the moistened version of the equivalent circuit model given above.

Interface impedances, for example, the double layer impedance effect, were ignored in the finite simulation model. While COMSOL does support parametrised boundary impedances, no suitable data was available which that facet of the model could be based upon.

The model was 20 cm long and 10 cm wide, approximating an adult's forearm. The electrodes were modelled as two, 2–d squares, 28 × 28 mm in size, of variable distance apart, centred at the top of the *stratum corneum*. One of these squares was tied to ground, the other given a 1 V sinusoidal input signal, at frequencies from 1 Hz to 1 MHz. Simulations was repeated with the electrodes 3, 5, 7 and 9 cm apart, as with the physical tests.

The model was divided into its elements using COMSOL's 'extra fine' meshing setting, producing elements no larger than 4 mm in size.

As well as measuring the impedance with this default model, versions were tested with the thickness of each layer increased and then decreased by 10% in turn. This was done to assess the sensitivity of the results to the inevitable variations in skin layers that exist between different areas of the body and between different people.

Similarly, a version was constructed which, instead of having the interfaces between layers flat, replaced them with sinusoidally oscillating surface, as shown in figure 7 (centre). The wavelength of these oscillations was 2 cm, creating 10 oscillations across the length of the model. Even with these modifications, the model is not a perfect representation of the geometry of the skin, but adding these oscillations is a

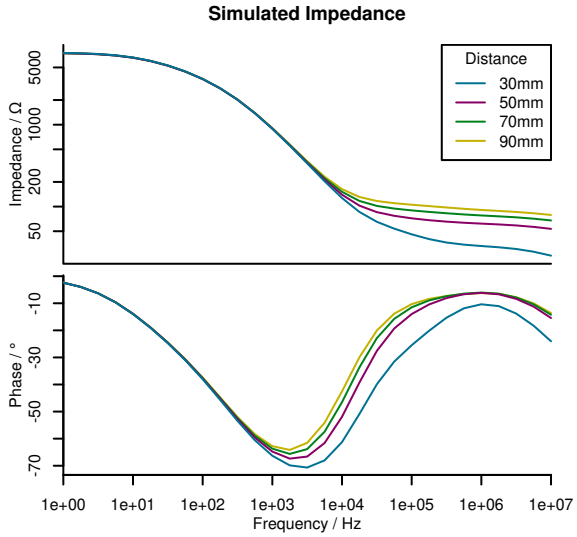

Figure 8. Simulated impedance spectrum between two electrodes on skin at 4 different distances. Low frequencies face a large impedance of around 7.5 kΩ, unaffected by changing distance. Higher frequencies show less than 100 Ω when the electrodes are 9 cm apart, falling as low as 25 Ω at 3 cm.

practical way of gauging the inaccuracies caused by the model's simplifications.

3.2. Finite Element Model Results

The impedance between electrodes in the standard version of the model is shown in figure 8. The overall shape of the impedance curve is as expected: low frequencies face a large resistive impedance that is not affected by the distance between electrodes. As the frequency of the input is increased, the impedance decreases as current is able to pass the *stratum corneum*. What remains is a smaller impedance that is affected by distance: the result of the lower tissues.

Varying the thickness of each layer, the results of which are shown in figure 9, confirms this interpretation. Changing the thickness of the *stratum corneum*, induced a proportional change in the impedance at low frequencies, while having very little effect on the high frequency impedance. Changing the thickness of the dermis, the most conductive of the layers, had an equivalent effect on the higher frequencies.

Creating oscillations in the boundary between layers causes changes across the whole frequency spectrum (figure 10). Creating a shortcut across the *stratum corneum*, reduces the low frequency impedance, in much the same way that changing the thickness did. Changes in the high frequency impedance are also caused as the effective resistance and capacitance of each layer changes.

These two tests can be used to draw conclusions about the reliability of the model. The fact that changing the heights of the tissue layers causes only a small change in the model's output indicates that errors in the data on layer thicknesses

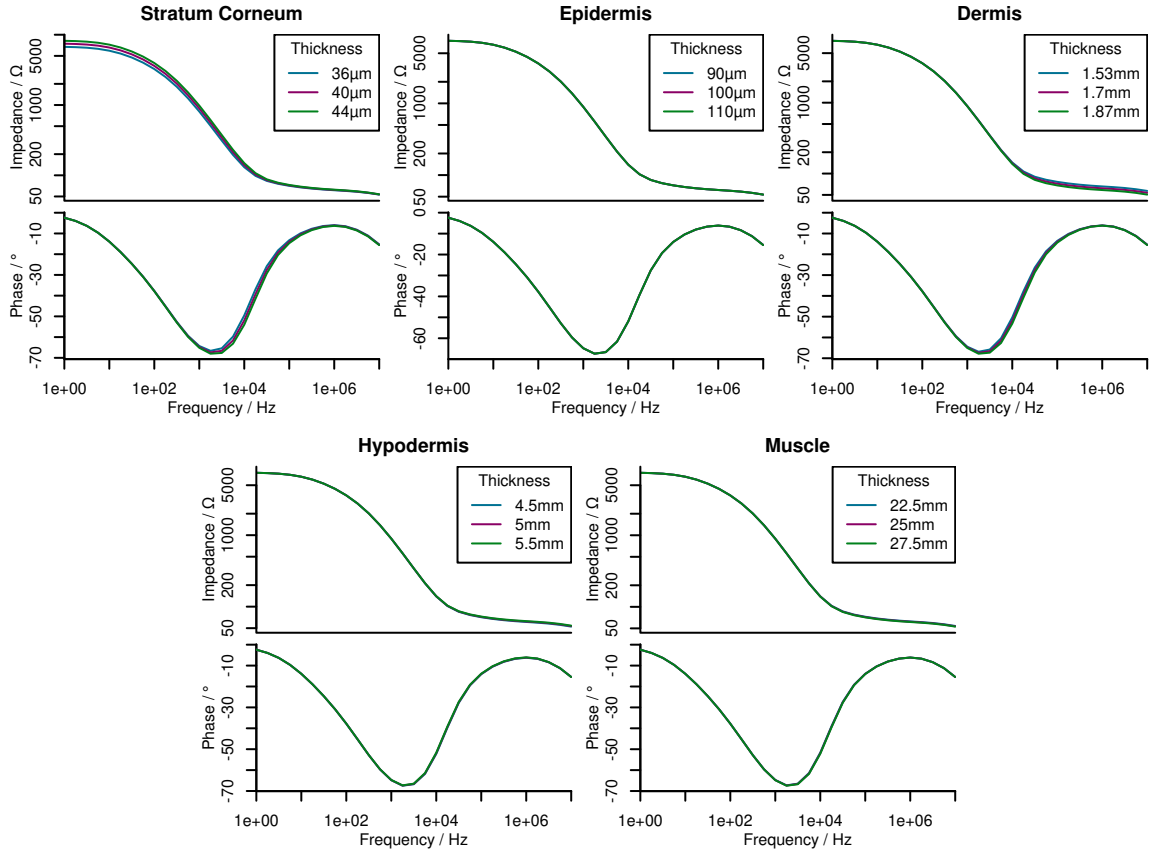

Figure 9. Simulated tissue impedance with varied layer thicknesses. Changing the thickness of most layers has only a very minor effect. The exceptions are the *stratum corneum* which affects the low frequency impedance, and the dermis which affect the value at high frequencies.

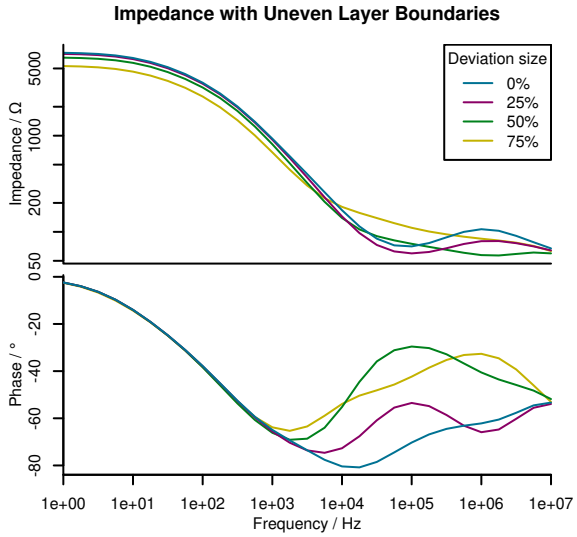

Figure 10. Simulated impedance between two electrodes, 5 cm apart, when the boundary between layers varies by 0, 25, 50 or 75% the height of the layer above it.

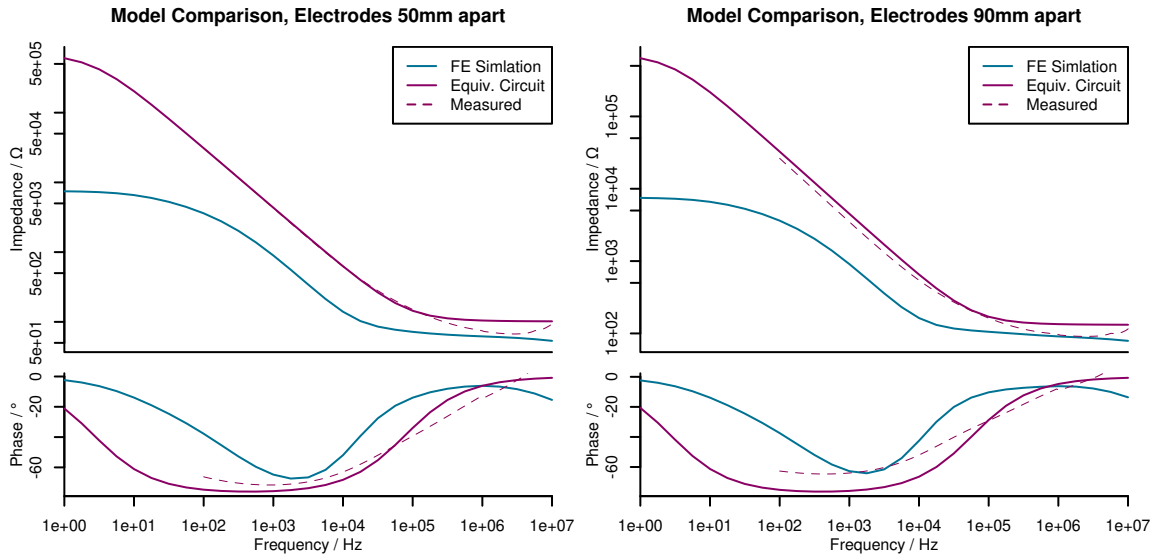

Figure 11. Simulated impedance results from the two models with the electrodes 50 mm (left) and 90 mm apart (right). The equivalent circuit plot is calculated from the 50 g, wet case, as this was closest, reliably derived case to the finite element simulation results and because the finite element model was derived from data collected on wet skin. The average of the measured plots, from which the equivalent circuit model was derived, is also given.

would not greatly impact the model's predictions. Conversely, the larger effect changing the layer boundary shape has on the results at high frequencies means that, if accurate predictions about the tissue's high frequency impedance are needed, accurate information about the layer boundary topography would be required.

4. Comparison of Finite Element and Equivalent Circuit Models

A comparison of the two models is shown in figure 11. While they are in approximate agreement about the impedance at high frequencies and about how the impedance transitions from high to low, there is a large discrepancy in their predictions about low frequencies.

Some amount of this difference will result from the equivalent circuit's inclusion of the electrodes and double–layer interface impedances, which the COMSOL model lacks. However, the tests of the electrode's impedance on to a copper sheet showed that this should account for less than 1 kΩ, far less than the 50 kΩ required to explain the discrepancy. The double–layer impedance effect, meanwhile, primarily adds capacitance to material interfaces so its inclusion in the COMSOL model would only serve to separate the models further in their transition from high to low impedance.

The fact that the error is largest at low frequencies implies that it is associated with the modelling of the *stratum corneum*. The COMSOL model can be made to resemble the equivalent circuit by increasing the thickness of the *stratum corneum* from

40 µm to 400 µm. However, it is known with confidence that the *stratum corneum* on the ventral forearm is not this thick. A more likely explanation is that an inaccuracy exists in the electrical properties of the layer. These values can be difficult to measure given the layer's small size and the difficultly in isolating a sample as well as its propensity to change properties depending on how much moisture has been applied and whether any layers have been physically removed (Martinsen et al. 1997, Yamamoto & Yamamoto 1976). And because the electrical properties of the *stratum corneum* are dependent on the eight individual values shown in table 1, it is difficult to derive corrected values from these results alone.

5. Conclusions

Both the finite element simulation and the equivalent circuit model developed here, show the impedance between two electrodes to consist of a large resistive impedance at low frequencies, shifting to a decreasing capacitive impedance at 10 to 100 Hz. This is caused by the thin, low conductivity layers at the top of the skin.

The relationship between the impedance of the electrodes when placed on a copper sheet to the applied mass and the permittivity of the electrolyte, shown in figure 5, indicates that the capacitive component of the impedance is likely to arise, at least in part, from the electrolyte beneath the electrode rather from the electrode–electrolyte boundary or the electrode itself, as originally proposed. Aside from this, the physically measured impedance data, correlated well with that predicted by the model in figure 1 from Neuman (2010).

The two models disagree about the exact frequencies these changes occur at and, most drastically, about the total impedance at low frequencies. These differences indicate an error in the data used to model the *stratum corneum*.

Nevertheless, these models can be used to make predictions about how current passes through the tissue. For example they show that low frequency stimulation, below 100 Hz, will mainly deliver energy to the high resistance, outer layers of the skin, providing heating effects, but less neural perception. Higher frequencies, above 10 kHz will use the capacitive properties of the upper layers to penetrate deeper, delivering energy to the living tissues.

The equivalent circuit model also shows the effects of moisture and pressure on the different constituents of the impedance. This is important when considering the differences between traditional, gel based electrodes and dry electrodes suitable for long term use.

Ethics Statement

Ethical approval was obtained from the University of Southampton (study ID: 64238) before conducting tests on human participants.

The research was undertaken in accordance with the Declaration of Helsinki. All subjects were over 18 and gave written, informed consent.

Funding Acknowledgement

This work was funded by EPSRC project reference 2280784.

Data Availability

The COMSOL models, recorded data and analysis scripts are available at `https://doi.org/10.5258/SOTON/D2487`

References

Archer D G & Wang P 1990 The dielectric constant of water and debye-hückel limiting law slopes *Journal of Physical and Chemical Reference Data* **19**(2), 371–411. *doi:10.1063/1.555853*

Assambo C, Baba A, Dozio R & Burke M J 2007 Determination of the parameters of the skin-electrode impedance model for ecg measurement *in* 'Proceedings of the 6th WSEAS Int. Conf. on Electronics, Hardware, Wireless and Optical Communications' pp. 90–95.

Birgersson U, Birgersson E, Nicander I & Ollmar S 2013 A methodology for extracting the electrical properties of human skin *Phisiological Measurement* **34**, 723–736. *doi:10.1088/0967-3334/34/6/723*

Brown B H, Smallwood R H, Barber D C, Lawford P V & Hose D R 1999 *Medical Physics and Biomedical Engineering* Taylor & Francis.

Cole K S & Cole R H 1942 Dispersion and absorption in dielectrics ii. direct current characteristics *The Journal of Chemical Physics* **10**(2), 98–105. *doi:10.1063/1.1723677*

Gabriel C, Gabriel S & Corthout E 1996 The dielectric properties of biological tissues: I. literature survey *Physics in Medicine and Biology* **41**, 2231–2249. *doi:10.1088/0031-9155/41/11/003*

Gabriel S, Lau R W & Gabriel C 1996 The dielectric properties of biological tissues: III. parametric models for the dielectric spectrum of tissues *Physics in Medicine and Biology* **41**, 2271–2293. *doi:10.1088/0031-9155/41/11/003*

Hartinger A E, Guardo R, Kokta V & Gagnon H 2010 A 3-d hybrid finite element model to characterize the electrical behavior of cutaneous tissues *IEEE Transactions on Biomedical Engineering* **57**(4), 780–789. *doi:10.1109/TBME.2009.2036371*

Holbrook K A & Odland G F 1974 Regional differences in the thickness (cell layers) of the human stratum corneum *The Journal of Investigative Dermatology* **62**(4), 415–422. *doi:10.1111/1523-1747.ep12701670*

Huclova S, Erni D & Fröhlich J 2010 Modelling effective dielectric properties of materials containing diverse types of biological cells *Journal of Physics D: Applied Physics* **43**. *doi:10.1088/0022-3727/43/36/365405*

Kaczmarek K & Webster J 1989 Voltage-current characteristics of the electrotactile skin-electrode interface *in* 'Images of the Twenty-First Century. Proceedings of the Annual International Engineering in Medicine and Biology Society' pp. 1526–1527. *doi:10.1109/IEMBS.1989.96322*

Lahtinen T, Nuutinen J & Alanen E 1997 Dielectric properties of the skin *Physics in Medicine and Biology* **42**, 1471–1472. *doi:10.1088/0031-9155/42/7/020*

Lee Y & Hwang K 2002 Skin thickness of korean adults *Surgical and Radiological Anatomy* **24**, 183–189. *doi:10.1007/s00276-002-0034-5*

Li Z 2018 'Textile electrode design and simulation for bio-signal recording'. URL: *https://eprints.soton.ac.uk/433540/*

Liu M, Ahmed Z, Grabham N, Beeby S, Tudor J & Yang K 2022 An all dispenser printed electrode structure on textile for wearable healthcare *in* '3rd International Conference on the Challenges, Opportunities, Innovations and Applications in Electronic Textiles'. *doi:10.3390/engproc2022015016*

Liu M, Beeby S & Yang K 2019 Electrode for wearable electrotherapy *in* 'International Conference on the Challenges, Opportunities, Innovations and Applications in Electronic Textiles'. *doi:10.3390/proceedings2019032005*

Martinsen Ø G, Grimnes S & Sveen O 1997 Dielectric properties of some keritanised tissues. part 1: Stratum corneum and nail in situ *Medical and Biological Engineering and Computing* **35**, 172–176. *doi:10.1007/BF02530033*

Neuman M 2010 Biopotential electrodes *in* J Webster, ed., 'Medical instrumentation: application and design' 4th edn Wiley chapter 5, pp. 189–240.

Pliquett U, Langer R & Weaver J C 1995 Changes in the passive electrical properties of human stratum corneum due to electroporation *Biochimica et Biophysica Acta* **1239**, 111–121.

R Core Team 2022 *R: A Language and Environment for Statistical Computing* R Foundation for Statistical Computing Vienna, Austria. URL: *https://www.R-project.org*

Schwan H P 1957 Electrical properties of tissue and cell suspensions *in* J. H Lawrence & C. A Tobias, eds, 'Advances in Biological and Medical Physics' Vol. 5 pp. 147–209.

Spinelli E, Pallas-Areny R & Mayosky M 2003 Ac-coupled front-end for biopotential measurements *IEEE Transactions on Biomedical Engineering* **50**(3), 391–395. *doi:10.1109/TBME.2003.808826*

Stuchly M A & Stuchly S S 1980 Coaxial line reflection methods for measuring dielectric properties of biological substances at radio and microwave frequencies - a review *IEEE Transactions on Instrumentation and Measurement* **IM-29**(3), 176–183. *doi:10.1109/TIM.1980.4314902*

Taji B, Shirmohammadi S & Groza V 2014 Measuring skin-electrode impedance variation of conductive textile electrode under pressure *in* '2014 IEEE International Instrumentation and Measurement Technology Conference (I2MTC) Proceedings'. *doi:10.1109/I2MTC.2014.6860909*

Taji B, Shirmohammadi S, Groza V & Batkin I 2014 Impact of skin–electrode interface on electrocardiogram measurements using conductive textile electrodes *IEEE Transactions on Instrumentation and Measurement* **63**(6), 1412–1422. *doi:10.1109/TIM.2013.2289072*

Tankisi H, Burke D, Cui L, de Carvalho M, Kuwabara S, Nandedkar S D, Rutkove S, Stålberg E, van Putten M J & Fuglsang-Frederiksen A 2020 Standards of instrumentation of emg *Clinical Neurophysiology* **131**(1), 243–258. *doi:https://doi.org/10.1016/j.clinph.2019.07.025*

Xiong F, Chen D, Chen Z, Jin C & Dai S 2019 Impedance characteristics of the skin-electrode interface of dry textile electrodes for wearable electrocardiogram *in* G Fortino & Z Wang, eds, 'Advances in Body Area Networks I' Springer International Publishing pp. 343–356.

Yamamoto T & Yamamoto Y 1976 Electrical properties of the epidermal stratum corneum *Medical and Biological Engineering* **14**, 151–158.